International Journal of Steel Structures 16(4): 1355-1363 (2016)
DOI 10.1007/s13296-016-0086-8
ISSN 1598-2351 (Print)
ISSN 2093-6311 (Online)

International Journal of
STEEL
STRUCTURES
www.springer.com/journal/13296

Finite Element Analysis of Optimized Brace Angle for the Diagrid Structural System

YongJae Lee[1], Jintak Oh[2], Hussam Hassan Abdu[3], and Young K. Ju[1,*]

[1]*School of Civil, Environmental and Architectural Engineering, Korea University, Seoul, Korea*
[2]*Inspection Division, Korea Infrastructure Safty & Technology Corporation, Jinju, Korea*
[3]*Technical Affairs, king Saud Bin Abdulaziz University for Health Science, Jeddah, Saudi Arabia*

Abstract

The Diagrid structural system is considered to be the best structural system for constructing free form structures, but it is also a very effective system for resisting lateral load. As a newly investigated structural system, its complicated node has not yet been completely investigated, and only minimal experimentation with the manufacturing and construction of the system has been conducted. Therefore, the construction cost of the diagrid structural system is still comparatively high. In this study, the cyclic performance of a diagrid node with an H-section brace is discussed with an emphasis on the welding methods, overlapped length, and diagrid angle. Details considering productivity were proposed, and their structural performance was assessed through experimental and analytical investigation.

Keywords: FEM, Diagrid, Cyclic test, Analysis

1. Introduction

Construction of tall buildings began in the 19th century. At first, tall buildings referred to buildings that were higher than others. But in recent years, the term refers to buildings that are taller than 100 m. Especially, many tall buildings have been built in Asia during the last 10 years. Over the past decade, tall buildings have been designed to not only account for height but also a free-form shape. This trend has already been discussed in the Council on Tall Buildings and Urban Habitat (CTBUH) 2006 World Conference in Chicago. The major topic of the conference was "Thinking outside the Box: Tapered, Twisted, Tilted Towers" (Kim *et al.*, 2009; Kim and Ju, 2010). 3T (Tapered, Twisted, Tilted) designs have been suggested for free-form shaped buildings. So, free-form shaped tall buildings have become a landmark in cities and many clients want a free-form building.

For this reason, new structural systems have been developed for free-form structures. The diagrid structural system is the most famous free-form structure. (Moon and Ali, 2007; Moon *et al.*, 2007; Kim *et al*., 2009, Kim *et al*., 2010; Lee *et al.*, 2015).

A free-form shape building is required a review of seismic performance. When earthquake occurred, a free-form shape building can be collapsed by eccentric mass form tapered, tilted and twisted. Therefore, seismic performance evaluation of diagrid structure is one of the important elements in structural design. The diagrid structural system is a very efficient system for both cases. Thus, the diagrid structural system has a double advantage for tall buildings; good resistance to loads and free-form shapes.

The diagrid is a mixed word composed of diagonal and grid. The diagrid structural system consists of triangular modules without vertical columns. It is more difficult than X-brace and K-brace structural systems. The triangular module is made of two braces and one beam. This system is resistant to lateral load due to the braces. When a lateral load occurs, the braces resist the associated tensile and compressive forces. The beam restrains the braces. A change in the diagonal brace length and angle can result in a differently shaped triangle module. The diagrid structural system can create a free-form shaped building through the combination of different triangular module shapes. Therefore, the diagrid structural system has various node shapes (Fig. 1). Each node shape and angle is different; Mary Axe uses circular steel tubes, CCTV uses rectangle sections, Capital Gate Tower uses boxed sections, and Macquarie Bank uses H-section. Many researchers have studied the shape and angle of diagrid nodes (Moon and Ali, 2007; Moon *et al.*, 2007; Kim *et*

Received February 19, 2016; accepted September 4, 2016;
published online December 31, 2016

*Corresponding author
Tel: +82-2-3290-3327, Fax: +82-2-928-7656
E-mail: tallsite@korea.ac.kr

(a) 30st. Mary Axe (b) CCTV (c) Capital Gate Tower (d) Macquarie Bank

Figure 1. Diagrid nodes.

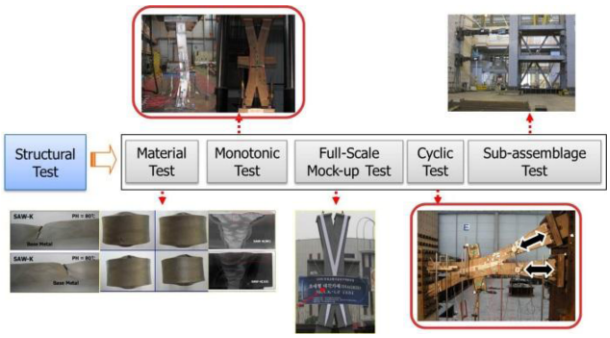

Figure 2. The process of Diagrid experiments.

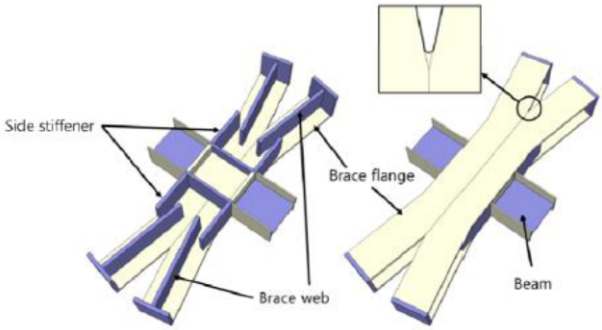

Figure 3. 3D view of specimen.

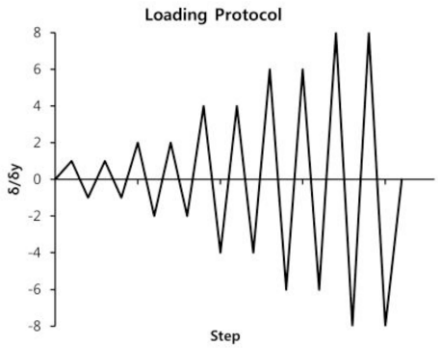

Figure 4. Loading protocol.

al., 2009, Kim *et al*., 2010; Lee *et al.*, 2015).

Moon *et al*. (2007) reported that the optimum angle of diagrid nodes was 60 degrees. Their results were limited to analysis of the 2D-model and did not include actual tests of the diagrid node (Moon and Ali, 2007; Moon *et al.*, 2007).

Structural performance analysis of the diagrid node is required for inelastic analysis of the seismic design, because the diagrid node has a very complex behavior due to the number of components (2 beam, 4 brace) connected at one node (Kim and Lee, 2008; Kim and Lee, 2009; Kim and Ju, 2009, Xiaolei *et al.*, 2008).

For the structural performance evaluation of the diagrid node, a series of tests was conducted, supported by the Korea Institute of Construction and Transportation Technology Evaluation and Planning (Kim *et al.*, 2009; Kim and Ju, 2010). With this support, a material test, monotonic tensile/compressive test, mock-up test, cyclic test, and frame test were conducted and the results are illustrated in Fig. 2. Among these tests, the cyclic test will be discussed in this paper, including further research on the test. The seismic performance of diagrid nodes with H-section braces was assessed through experimental and analytical studies. The analysis was conducted using the same condition as that of the cyclic test, and the results matched well with the test results. The generalized behavior of the diagrid node was then derived by expanded parameter analysis.

2. Experimental Study

2.1. Test specimen

The diagrid nodes that were to be tested were selected from the lowest node of the Lotte Super Tower (112 floors) in Seoul. The Lotte Super Tower is 555 meter tall with a 70 square meter footprint formed by two intersecting 39 meter diameter circular arcs. The structural system of this building is comprised of a reinforced concrete core wall and a steel perimeter diagrid frame. The node used in the experiment is subjected to the most stress in the tower. Tests on that the nodes were introduced in preceding research (Kim *et al.*, 2009; Kim and Ju, 2010). In Chapter 2, a brief introduction of the experimental research is presented followed by comparison with FEM

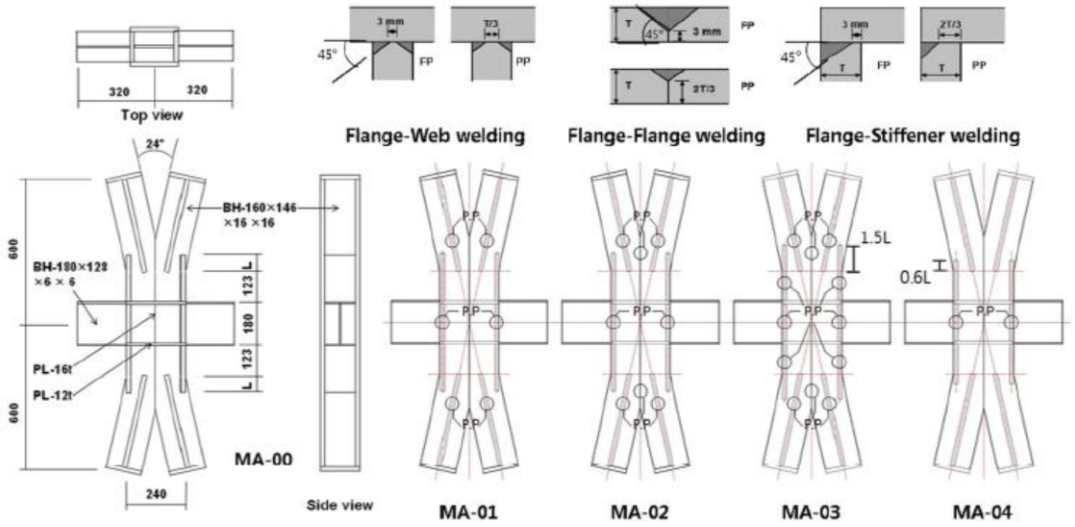

Figure 5. Details of parameters.

analysis in Chapter 3.

Figure 3 shows a 3D image of the test specimen. The X-shaped node at which the H-section braces intersect has a continuous flange and a transferred web. Through the transferring zone, the axial stress of the web flows to the side stiffener.

The parameters of the web-transferred node are the overlapped length between the side stiffener and web and the welding method used for the major parts. The stress transferring efficiency of the transferring zone depends on the overlapped length; therefore, the structural performance of the node with respect to the overlapped length was determined. For tall buildings, very thick plates and a considerable amount of welding are needed to manufacture the diagrid nodes. If partial penetration welding (which reduces the amount of welding required) can be applied when manufacturing the nodes, the total welding amount would decrease significantly. Therefore, the partial penetrating welding method is introduced as a parameter.

Five specimens are illustrated in Fig. 5. The MA-00, MA-01, and MA-02 specimens have the same form, with an overlapped length of 70 mm, while their welding methods differ. The MA-03 and MA-04 specimens have an overlapped length of 105 and 42 mm, respectively.

2.2. Test setup

To simulate the conditions under lateral load, a tensile force is applied to one brace and a compressive force is applied to the other brace. The angle between the two braces is 24 degrees and is scaled to 1/5. Forces are applied twice in one cycle and the magnitude is increased as the axial deformation of the brace reaches. The yield displacement (δ_y=2 mm) corresponding to the yield strength (2940 kN) and this yield displacement was incremented at 2 mm (δ_y), 4 mm (2 δ_y), 8 mm (4 δ_y), and 12 mm (6 δ_y), which is one, two, four, and six times the yield displacement, respectively (Fig. 4). The tests are completed when the specimens fracture or when the applied load decreases to 80% of the maximum strength. Fig. 6 shows the test set-up.

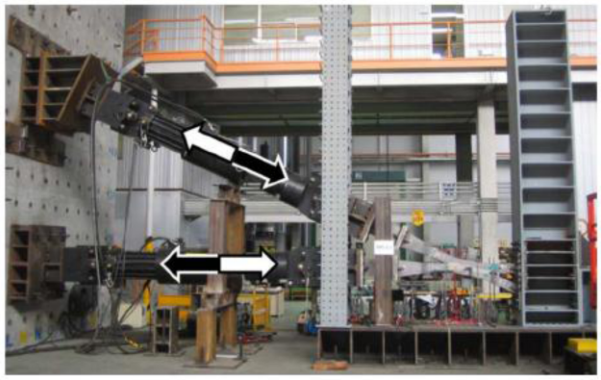

Figure 6. Test set-up.

2.3. Test results

Steel grade SM490 was selected for the specimens. According to the tensile tests, all specimens had higher yield strength than the standard strength (=325 MPa), and showed yield ratios ranging from 68% to 81% as well as elongation ranging from 23% to 29%. Fig 8 shows the measured cyclic response of MA-00 in the axial direction of the diagonal braces. In Fig. 6, the graph illustrates the load-displacement relationship of the upper diagonal brace (Fig. 7(a)) and that of the lower diagonal brace (Fig. 7(b)). When the upper diagonal brace was loaded in tension, the lower diagonal brace was loaded in compression.

The major failure mode is as follows: the combination of tensile and compressive forces, which have an angle of 24 degrees, causes vertical displacement of the node center (Fig. 7(c)). This displacement leads to extra moment,

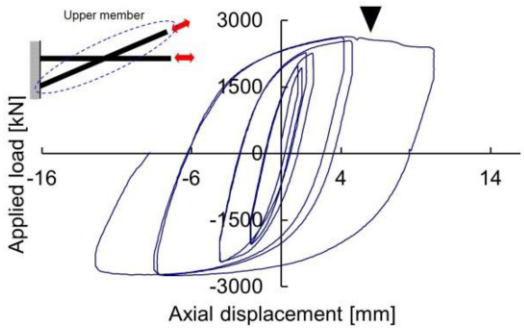

(a) MA-00 Upper

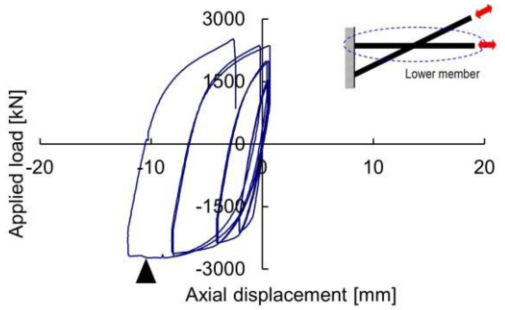

(b) MA-00 Lower

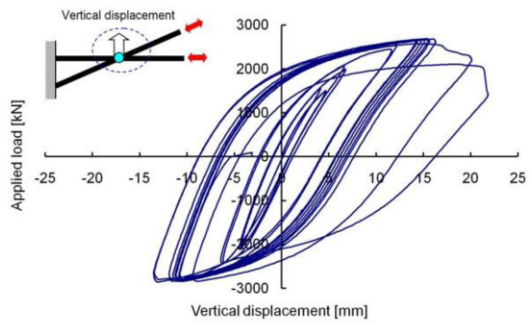

(c) MA-00 Center

Figure 7. Load-displacement.

which is the main reason for the crack in the flange. The test results are summarized in Fig. 8 and Table 1. According to the results, the welding method has no effect on initial

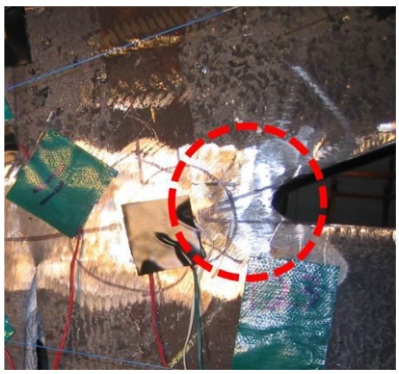

Figure 9. V-point.

stiffness. The MA-00 specimen has slightly higher initial stiffness than the MA-01 and MA-02. The MA-00 has full penetration welding. The MA-01 and MA-02 have partial penetration welding. The MA-03 specimen has higher stiffness than the MA-04 specimen. This means that the initial stiffness increases as the overlapped length increases. The yield strength is also affected by the overlapped length. The MA-03 specimen has higher yield strength than MA-04. No significant differences were found between MA-00, MA-01 and MA-02.

The strain on the edge of the flange is larger than that of the center and reaches yield strain early. The failure of the steel plate occurred at the V-point after the brace member buckled. Figure 9 shows the full penetration welding at the V-point. The failure in the V-point did not occur with the full penetration welding. Experimental results led to the conclusion that the V-point should be made with the full penetration welding.

3. Finite Element Analysis

3.1. Modeling

The parameters are the overlapped length between the side stiffener and web and the welding method used for the major parts. Kim *et al*. (2009) investigated the use of full penetration welding for the diagrid nodes. Also, they

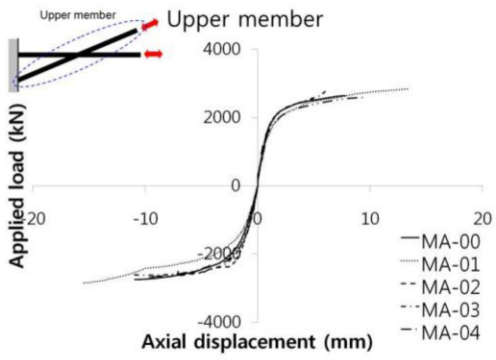

(a) Upper member

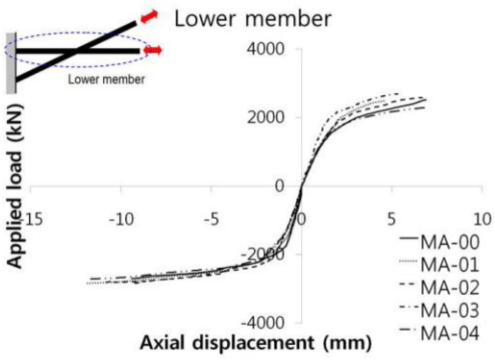

(b) Lower member

Figure 8. Skeleton curve.

Table 1. Test results

Specimens	Initial Stifiness [kN/mm]	Yield strength [kN]	Ductility	Energy dissipation [kN·m]
MA-00	1,914	2,017	6.73	304
MA-01	1,812	2,143	7.95	353
MA-02	1,646	2,112	5.70	340
MA-03	1,975	2,318	6.66	289
MA-04	1,428	1,828	9.71	410

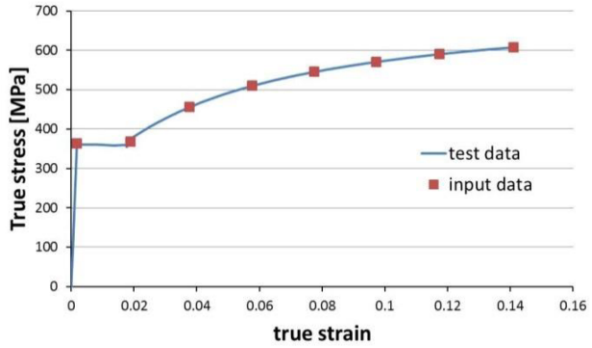

Figure 10. Material property.

Table 2. Tensile coupon test results

Specimens	Yield strerss [MPa]	Tensile stress [kN]	Yield ratio [%]	Elongation [%]
Plate-6	421	518	81	304
Plate-12	378	542	7.95	353
Plate-16	357	528	5.70	340

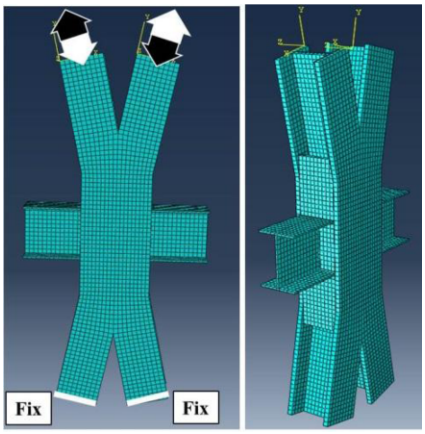

Figure 11. FEM model (MA-78).

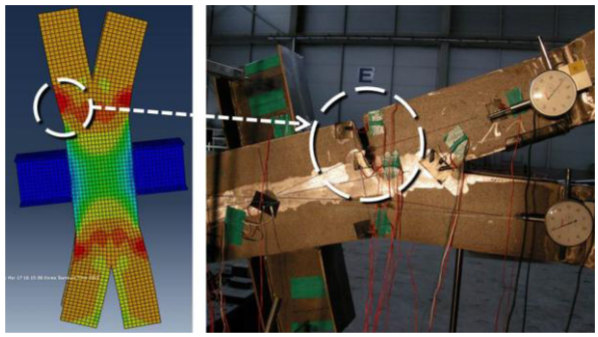

Figure 12. Failure point of model and specimen.

investigated the structural performance of the diagrid nodes (Kim *et al*., 2009; Kim and Ju, 2010). Based on the experimental results, the structural performance of the nodes has various angles that can be investigated through FEM analysis. The reliability of the analysis data was reviewed by comparing the test specimens and analysis models.

The MA-00 is a baseline specimen with a 78 degree brace angle. So, the analysis model, MA-78 is designed to be similar to MA-00. The same conditions as those of the test were used for the analysis and the Abaqus/CAE 6.10 program was used. All elements were designed using solid elements and the material properties of the coupon test were used (Fig. 10). The material used for all elements was SM490 steel (F_y =325 MPa, F_u =490 MPa). The young's modulus and Poisson's ratio obtained from the general steel properties of the materials are 210,000 MPa and 0.3 respectively (Daniel Y. Abebe *et al.*, 2015; Feng Zhou *et al.*, 2013; Girao Coelho *et al.*, 2006; Kim and Ju, 1999; Lee *et al.*, 2015; Oh and Ju, 2016; Ju *et al.*, 2013; Kim, Dargush and Ju, 2013).

The stress strain relationship used is obtained from coupon test (Table 2). This test also shows that the yield strength is 378 MPa and the ultimate strength is 542 MPa. This means, the yield strength and the ultimate strength of the material is around 16 and 10% higher than the corresponding strength used in the model. In order to consider the strain hardening effect in the analysis, the stress-strain relationship was taken as a multi isotropic hardening curve.

All instances were assembled using a tie interaction method. All elements of the diagrid node were meshed by the 4-node tetrahedral structural solid element C3D8. Figure 11 shows the boundary condition of the analysis model.

3.2. Comparison with experimental result

A comparison between the FEM analysis (MA78) and the experimental result (MA-00) are shown in Fig. 13. With monotonic-load (Fig. 13(a)), the yielding strength of the models is 2,017 kN (MA-00) and 1,989 kN (MA-78). With cyclic-loads (Fig. 13(b), differences occur in the 8th cycle. Failure occurred at the flange of the MA-00 specimen.

The same location in the analysis model reached maximum stress (Fig. 12).

As a result, the FEM model may be considered to be reliable for investigating the structural performance of various node angles under the same conditions (boundary, loading protocol, material property etc.).

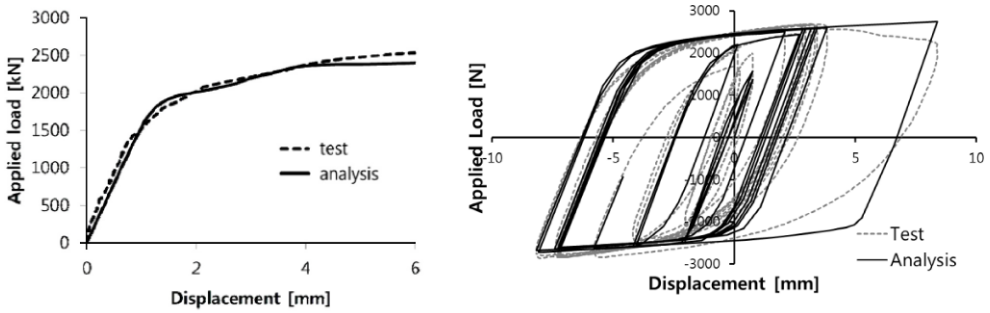

(a) Monotonic load (b) Cyclic load

Figure 13. Comparison between experimental and analysis for axial-load.

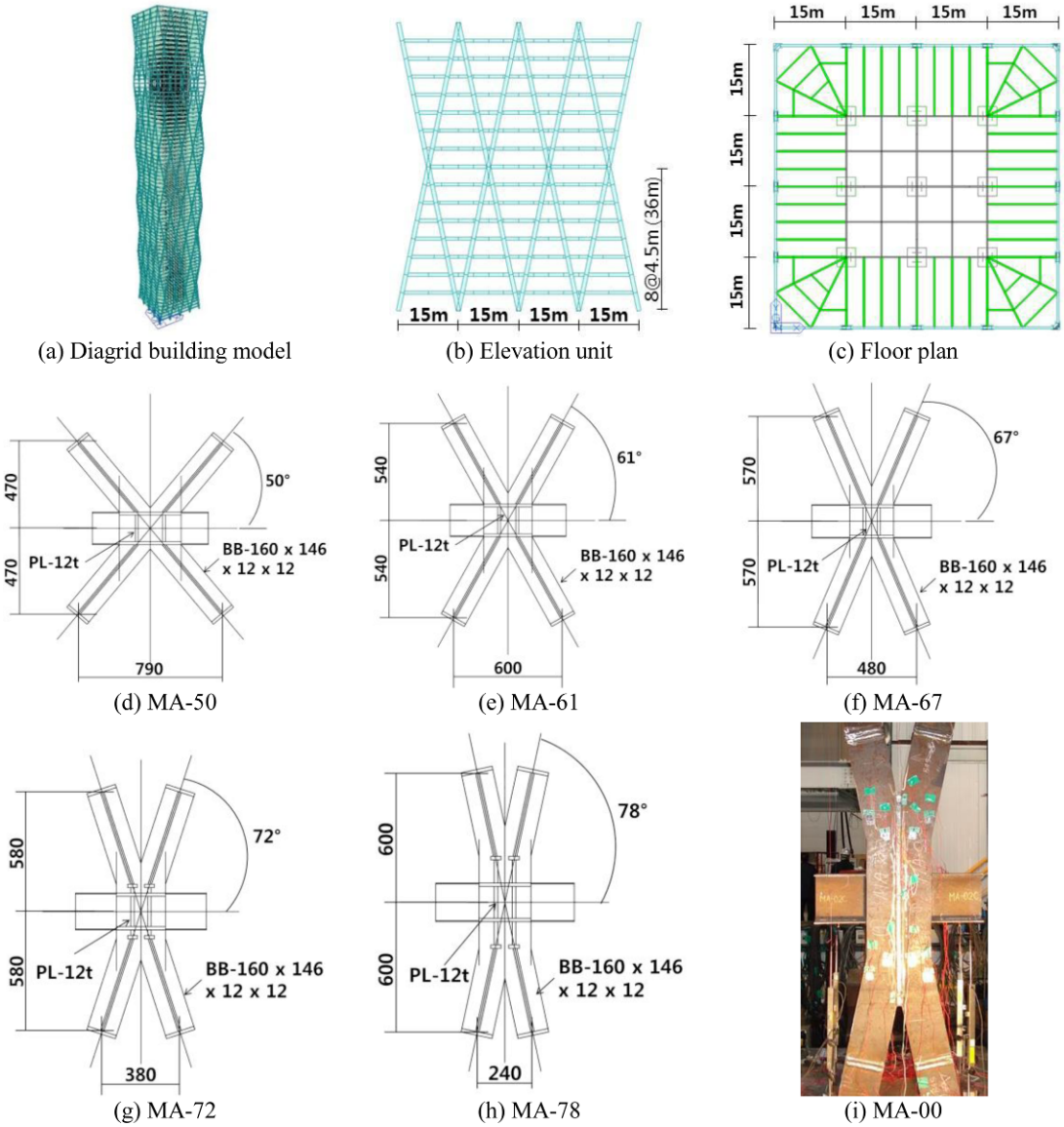

(a) Diagrid building model (b) Elevation unit (c) Floor plan

(d) MA-50 (e) MA-61 (f) MA-67

(g) MA-72 (h) MA-78 (i) MA-00

Figure 14. Analysis model design.

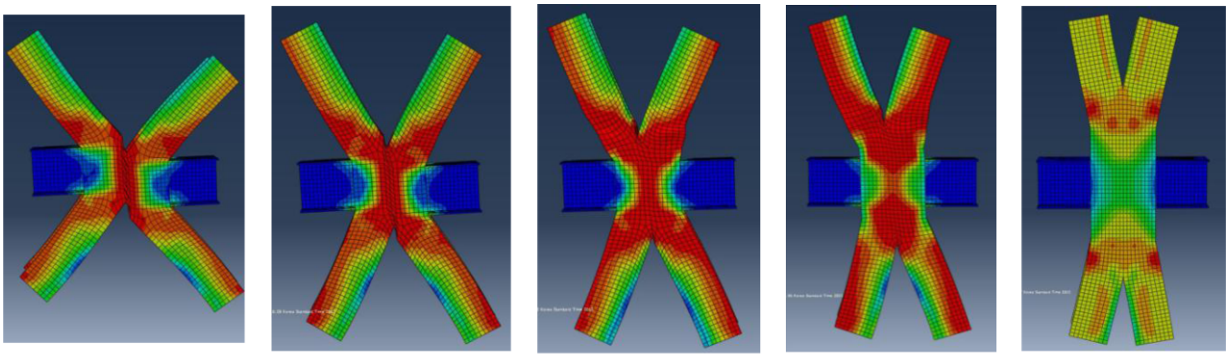

(a) MA-50 (b) MA-61 (c) MA-67 (d) MA-72 (e) MA-78

Figure 15. Analysis results without reinforcement at V-point.

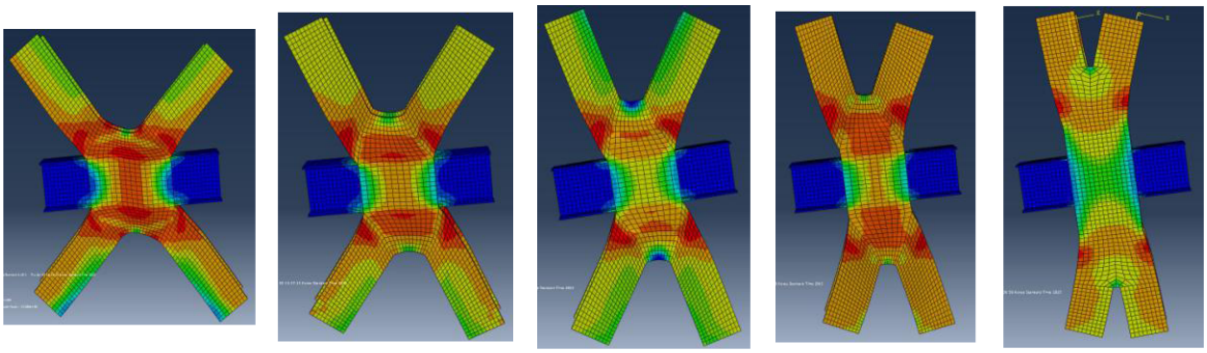

(a) MA-50C (b) MA-61C (c) MA-67 C (d) MA-72 C (e) MA-78 C

Figure 16. Analysis results with reinforcement at V-point.

4. Optimized for the Diagrid Node

4.1. General

Analysis of an 80-story building was planned due to the lateral load effect. The shape of the building is similar to that of the Hearst Tower (New York, 2006). So, the analyzed building has same four vertically elevated shape. This is because all diagrid nodes should cover a lateral load equally.

The design was checked for strength using the KBC code and found to be acceptable. The document KBC 2009 (*Korean Building Code*) is used to establish the wind load. The buildings are assumed to be category A buildings in Seoul, which implies that there is a substantial hazard to human life in the event of failure. Based on the code, the basic wind speed is 30 m/s.

4.2. Parametric study

The diagrid module was composed of the MA-78 model, and the elevation of the building comprised 40 repeated modules. The locations of the nodes should be matched on the floor (Moon and Ali, 2007; Moon *et al.*, 2007). Therefore, the 78, 72, 67, 61 and 50 degree parameters of the diagrid node were selected under the given design condition (Fig. 14(d), (e), (f), (g) and (h)). The analysis models were named MA-78, Ma-72, Ma-67, MA-61 and Ma-50, respectively. According to the results of the experiment, the brace behaved like a column. Therefore, the length of all diagonal braces was 1,260 mm to control for buckling.

4.3. Analysis results

The analysis models were subjected to cyclic loading of the AISC loading protocol. Similarly, experiment specimens were subjected to the same cyclic loading protocol. Figure 15 shows the details of the analysis results. The stresses on analysis models MA-78, 72, and 67 were concentrated around regions where higher stress occurred in experimental specimens. In contrast, immoderate vertical deformation occurred in the center part of the MA-61 and MA-50. This difference is due to the longer moment arm in MA-61 and MA-50. So, the larger stress occurred at the V-point, which caused shear deformation in the center flange. To decrease the shear deformation, it was necessary to reinforce the V-point, which is the part between each brace. Therefore, the V-points of all analysis models were reinforced with full penetrated welding and analyzed again. This was exactly the same condition as the experiment specimens.

4.4. Optimized brace angle

Figure 16 shows the analysis results of the diagrid node

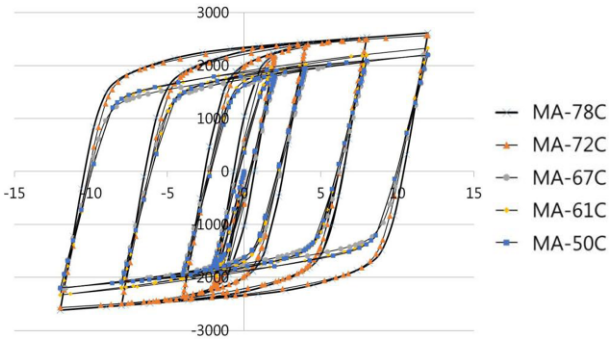

Figure 17. Load-displacement relationship.

Table 3. Summary of analysis result according to angle

Model	Initial Stiffness [kN/mm]	Ultimate Strength [kN]	Energy Dissipation [kN·m]
MA-50C	1,066	2,196	220 (80.29%)
MA-61C	1,131	2,329	227 (82.85%)
MA-67C	1,137	2,209	219 (79.93%)
MA-72C	1,385	2,568	259 (94.53%)
MA-78C	1,662	2,617	274 (100%)

with reinforced V-point, which has two different points, compared to the analysis results of the diagrid node with no reinforcement. In the former, shear deformation at the center of the node did not occur. This is because reinforcement of the V-point increases the area of the center flange. In the latter, failure of the diagrid node occurred as the brace buckled.

The maximum stress in the MA-78C with a reinforce V-point was discovered at the point where the brace and vertical stiffener meet. The experimental result of MA-00 is the same as the analysis stress result. Thus, the C-type analysis model with full penetrated welding at the V-point is the most accurate of the other diagrid node models.

Figure 17 shows the load-displacement relationship and the measured cyclic response of all models in the axial direction of the diagonal braces. When the upper diagonal brace becomes loaded with tensile force, the lower diagonal brace is loaded with compressive force.

The energy dissipations of MA-78C and MA-72C is 274 and 259 k·Nm respectively. Additionally, the energy dissipations of MA-67C, 61C, 50C is about 17.15~20.07 % less. Consequently, the upper 70 degrees of the diagonal braces is more efficient compared to the rest. This is because the force at the node acts like an axial force. The analysis results are summarized in Table 3. According to the results, the initial stiffness increases as the angle of the diagrid increases. The ultimate strength and energy dissipation are also affected by the angle of the diagrid.

5. Conclusion

In this research paper, the cyclic performance of a diagrid node with an H-section brace is discussed with an emphasis on the hysteresis characteristics, welding methods, and diagrid angle. Details that improve productivity were proposed, and the structural performance was assessed through experimental and analytical investigation.

(1) The test specimen (MA-00) was fractured by a crack in the flange where extra moment and tensile force were combined. This type of bending failure should be considered when designing a diagrid node.

(2) The results of theexperiment and FEM analysis both agree well; therefore FEM analysis may be useful for the diagrid node design. From the above results, reinforcement of the V-point will be needed during FE analysis of the diagrid node. V-point is a role for the reinforcement of the panel zone at the node center. But the size of the panel zone is different every five analysis model. So, it is impossible to compare the structural performance of the panel zone size effect.

(3) For a uniform angle in the diagrid structure, it was found that, as the angle increases, the performance of the diagrid node also increases because the aspect ratio tends to behave more like a bending beam, and steeper angle diagonals resist bending moments more efficiently through axial actions. Additionally, with angles below 67 degrees, the diagrid nodes have similar structural performance.

(4) The Lotte Super tower have 7.9 aspect ratio and 15 m node span. According to the structural design, the optimum angle is 78 degree. If the node span is longer than 15 m, the node angle can be more 78 degree. However, diagonal brace section becomes too large because of the risk of buckling. When considering the most economic section design, the optimal angle is 78 degree. From the above, it is apparent that a 72 degree angle for the diagrid node with an H-section is the optimum choice.

Acknowledgments

This work was supported by the National Research Foundation of Korea (NRF) grant funded by the Korea government (MSIP) (NO. 2013R1A1A2013578) and a grant (16AUDP-B100343-02) from Architecture & Urban Development Research Program funded by Ministry of Land, Infrastructure and Transport of Korean government.

References

Daniel Y. Abebe, Jeong, S.J, Jang J. H., Choi, J. H., Park, J. U. (2015). "Study on Inelastic Buckling and Residual Strength of H-Section Steel Column Member", *International journal of Steel Structures*, 15(2). pp. 365-374

Feng Zhou, Lewei Tong, Yiyi Chen (2013), "Experimental and numerical investigations of high strength steel welded h-section columns", *International journal of Steel Structures*, 13(2). pp. 209-218

Girao Coelho AM, Simoes da Silva L, Bijlaard FS. (2006). "Finite-element modeling of the nonlinear behavior of bolted T-stud connections." *Journal of Structural*

Engineering, 132(6), pp. 918-928

Ju, Y. K., Eom, T. S., Kim, J. H., Chang, I. H., Han, K. M., and An, S. M. (2007). "Structural performance of diagrid node." *Proc., Korean Society of Steel Construction*, KSSC, Seoul, 794-799.

Kim, S. D., Hong, W. K. and Ju, Y. K. (1999). "A modified dynamic inelastic analysis of tall buildings considering changes of dynamic characteristics." *The Structural Design of Tall Buildings*, 8(1), pp. 57-73

Kim, J. K. and Lee, Y. H. (2008). "Seismic performance evaluation of diagrid system buildings." *Journal of the Architectural Institute of Korea Structure & Construction*, 24(12), pp. 35-42.

Kim, J. K. and Lee, Y. H. (2009). "Seismic performance evaluation of diagrid system buildings." *Journal of the Architectural Institute of Korea Structure & Construction*, 25(6), pp. 13-20.

Kim, K. H., Ju, Y. K. and Kim, S. D. (2009). "Evaluation of seismic performance factors of diagrid structural system." *Journal of Korea Society of Steel Construction*, 22(3), pp. 229-239.

Kim, Y. J. et al (2010). "Cyclic behavior of diagrid nodes with H-section braces." *Journal of Structural Engineering*, 136(9), pp. 1111-1122

Kim, Y. J. et al (2011). "Experimental investigation of the cyclic behavior of nodes in diagrid structures." *Engineering Structures*, 33(7), pp.2134-2144

Kim, J. K., Dargush, Gary F., Ju. Y. K. (2013). "Extended framework of Hamilton's principle for continuum dynamics" *International Journal of Solids and Structures*, 50(20), pp.3418-3429

Lee, S. H., Lee, S. J., Kim, J. H. and Choi, S. M. (2015). "Mitigation of Stress Concentration in a Diagrid Structural System Using Circular Steel Tubes." *International journal of Steel Structures*, 15(3). pp.703-717

Moon, K. S., Connor, J. J., and Fernandez, J. E. (2007). "Diagrid structural systems for tall buildings: Characteristics and methodology for preliminary design." *The Structural Design of Tall and Special Buildings*, 16, pp. 205-230.

Moon, K. H. and Mir, M. Ali. (2007). "Structural developments in tall buildings: Current trends and future prospects." Architectural Science Review, 50(3), pp. 205-223

Oh, J. T., Ju, Y. K., Hwang, K. J.,Kim, S. D. and Lho, S. H. (2016). "FREE node for a single layer free-form envelope subjected to bending." *Engineering Structures*, 106, pp.25-35

Ju, Y. K., Kim, Y. C., Ryu, J. (2013) "Finite element analysis of concrete filled tube column to flat plate slab joint", *Journal of Constructional Steel Research*, 90, pp. 297-307

Xiaolei, H., Chao, H. and Jing, J. (2008) "Experimental and numerical investigation of the axial behavior of connection in CFST diagird structures", *Tsinghua Science and Technology*, 13(1), pp. 108-113